The Astronomical Journal, 134:223–228, 2007 July

SPECTROSCOPIC SEARCH FOR WATER ICE ON JOVIAN TROJAN ASTEROIDS

Bin Yang and David Jewitt
Institute for Astronomy, University of Hawaii, Honolulu, HI 96822, USA; yangbin@ifa.hawaii.edu, jewitt@hawaii.edu
Received 2007 February 2; accepted 2007 March 20

ABSTRACT

The Jovian Trojans likely formed beyond the snow line and so may contain considerable amounts of water ice. We seek near-infrared spectroscopic evidence for the 1.5 and 2.0 μm water ice bands in the Trojans. Our sample is focused on objects identified in previous measurements as being of special interest. The unusual Trojan (4709) Ennomos has a geometric albedo significantly above the mean Trojan albedo, perhaps because a recent impact has coated part of the surface with freshly excavated ice. Trojans (911) Agamemnon, (617) Patroclus, (1143) Odysseus, and (2797) Teucer were also observed. These objects have been independently reported to show possible weak absorptions at 1.7 and 2.3 μm, respectively. If real, the latter features may be due to organic materials present on the surfaces. However, all five targets appear spectrally featureless, even in our highest signal-to-noise ratio data. Simple models consisting of mixtures of water ice and a spectrally featureless material were used to quantify the limits to surface ice.

Key words: infrared: solar system — Kuiper Belt — minor planets, asteroids

1. INTRODUCTION

The Jovian Trojan asteroids are trapped in the L4 and L5 Lagrangian clouds of Jupiter, which lead and trail the planet by 60°, respectively. Their unique location, in the region between the inner rocky terrestrial bodies and the outer giant planets, gives us the opportunity to study an important transition zone in the solar system. The bulk compositions of Trojans are expected to relate to the conditions (i.e., temperature, pressure, and chemical composition) of the solar nebula at the time and the location of their formation. If the Trojans formed near where they are found today, they could provide important compositional clues about the core of Jupiter, itself thought to be an aggregate of icy planetesimals accreted from nearby orbits (Pollack et al. 1996; Fleming & Hamilton 2000). If the Trojans formed in the outer solar system and were subsequently scattered inward (Morbidelli et al. 2005), then their properties would instead be more representative of the Kuiper Belt objects (KBOs).

The likely source regions of the Trojans both lie beyond the so-called snow line, where the temperature in the solar nebula allowed water to condense out from the gas phase to form ice grains (Stevenson & Lunine 1988; Ciesla & Cuzzi 2006). Therefore, the Trojans are expected to be ice-rich. Water ice and hydrated minerals have been spectroscopically identified on other suspected water-rich objects, such as low-albedo asteroids (Jones et al. 1990; Lebofsky et al. 1990), Centaurs (Cruikshank et al. 1998; Luu et al. 2000; Doressoundiram et al. 2005), KBOs (Brown et al. 1997; Jewitt & Luu 2004), and comets (Davies et al. 1997; Kawakita et al. 2004). However, neither ices nor hydrated materials have been reliably observed on the Trojans with ground-based data, despite their supposedly water-rich heritage. Indeed, the spectra of the Trojans are remarkably featureless from optical to near-infrared wavelengths. Published optical reflectivity spectra are nearly linear, with spectral slopes that vary from neutral to moderately red (Jewitt & Luu 1990; Fornasier et al. 2004), while near-infrared spectra (Luu et al. 1994; Dumas et al. 1998; Emery & Brown 2003) show no indication of surface water ice. The optical geometric albedos of the Trojans are uniformly dark, with a mean value of 0.041 ± 0.002 (Fernández et al. 2003). These characteristics taken together are suggestive of an irradiated hydrocarbon surface (Moroz et al. 2004), although other interpretations are possible (Cruikshank et al. 2001).

A few objects have been reported to exhibit possible weak absorptions, which may be due to the presence of hydrocarbon species. For example, multiple spectra taken with different instruments on (1143) Odysseus show broad absorption at 1.7 μm (Emery 2002). Trojans (911) Agamemnon and (2797) Teucer also show a hint of this feature. A weak absorption in the 2.2–2.4 μm region has been suggested in *K*-band spectra of (2797) Teucer and (617) Patroclus (Emery 2002). Emery (2002) argued that because the transparency of the atmosphere is high in that wavelength region, this feature is unlikely to be caused by telluric absorption.

Trojan (4709) Ennomos was found to have an extraordinarily bright geometric albedo of 0.13 ± 0.02 (for beaming parameter $\eta = 0.94$, see Lebofsky & Spencer 1989) by Fernández et al. (2003). This value is significantly higher than the mean albedo of 32 Trojan asteroids measured in the same way, namely, $\bar{p}_v = 0.041 \pm 0.002$ (Fernández et al. 2003). The remarkably high albedo makes (4709) Ennomos a spectroscopically attractive target, since the unusual brightness might suggest the presence of surface ices, which could produce diagnostic features in the near-infrared. One intriguing hypothesis is that Ennomos experienced a recent impact, which penetrated through the dark carbonaceous mantle and exposed interior icy grains (Fernández et al. 2003).

In this paper, we investigate (4709) Ennomos, as well as the above four Trojans that have been tentatively reported to show absorption bands in the near-infrared. We attempt to test for the presence of water ice and to replicate the reported band detections.

2. OBSERVATION AND DATA REDUCTION

Observations were taken using the United Kingdom Infrared Telescope (UKIRT) 4 m and the NASA Infrared Telescope Facility (IRTF) 3 m telescopes atop Mauna Kea, Hawaii. We observed (4709) Ennomos on UT 2002 September 30 and 2002 October 1 and 3, using SpeX (Rayner et al. 2003), a medium-resolution 0.8–2.5 μm spectrograph on IRTF. SpeX is equipped with a Raytheon 1024×1024 InSb array with the plate scale of $0.12''$ pixel^{-1} and covers a $60'' \times 60''$ field of view. Spectra of (911) Agamemnon, (1143) Odysseus, and (2797) Teucer were taken on UT 2006 June 22–25, also using SpeX. The low-resolution prism (LoRes) mode in the wavelength range from 0.8 to 2.5 μm was used for all our observations on IRTF. A $0.5'' \times 15''$ slit was used for IRTF observations, which provided

TABLE 1
Observational Parameters

Trojan Asteroid	UT Date	V (mag)	α (deg)	Wavelength (μm)	Integration Time (s)	Air Mass	Standard	Telescope and Instrument
(4709) Ennomos	2002 Sep 30	16.63	11.0	0.8–2.5	120 × 8	1.01–1.00	HR 2141 G2	IRTF+Spex[a]
(4709) Ennomos	2002 Oct 1	16.62	11.0	0.8–2.5	120 × 12	1.01–1.00	HR 2141 G2	IRTF+Spex
(4709) Ennomos	2002 Oct 3	16.61	10.8	0.8–2.5	120 × 24	1.02–1.00	HR 2208 G2	IRTF+Spex
(617) Patroclus	2006 Apr 7	16.13	6.6	1.4–2.5	240 × 16	1.26–1.68	BS 4345 G0	UKIRT+UIST
(617) Patroclus	2006 Apr 8	16.13	6.7	1.4–2.5	240 × 16	1.05–1.20	BS 4459 G9	UKIRT+UIST
(911) Agamemnon	2006 Jun 25	15.18	6.3	0.8–2.5	120 × 6	1.88–1.95	HD 196746 G2	IRTF+Spex
(2797) Teucer	2006 Jun 23	15.8	4.1	0.8–2.5	120 × 10	1.90–2.06	HD 182465 G2	IRTF+Spex
(1143) Odysseus	2006 Jun 23	15.4	3.4	0.8–2.5	120 × 10	1.63–1.81	HD 182041 G2	IRTF+Spex
(1143) Odysseus	2006 Aug 14	15.6	6.1	1.4–2.5	240 × 6	1.43–1.50	HD 174466 G2	UKIRT+UIST

[a] The IRTF observations of (4709) Ennomos were made by S. Sheppard.

a spectral resolving power that varied with wavelength in the range of 90–210 (average $\lambda/\Delta\lambda = 150$). Spectroscopic observations of (617) Patroclus were taken on UT 2006 April 7 and 8 at UKIRT using UIST (Ramsay Howat et al. 2004), a 1–5 μm imager-spectrometer with a 1024×1024 InSb array. We used the HK grism and a 0.48″ wide, 120″ long slit. The average resolution was $\lambda/\Delta\lambda \approx 550$ over the 1.4–2.5 μm range. Additional observations of (1143) Odysseus were taken using UIST on UT 2006 August.

Target information at the time of the observations, as well as details of the instruments and observed standard stars, are summarized in Table 1.

We followed the standard spectroscopy data reduction procedure. A flat-field frame was created by averaging and normalizing a set of individual dome flat frames. Bad-pixel masks were created using bias and flat-field frames to identify and fix pixels with poor response. The pixel-to-pixel sensitivity variations were calibrated by dividing the master flat-field frame from the object frames. First-order sky removal was done by subtracting image pairs taken by nodding the object along the slit between two different positions separated by ~6″. However, airglow emissions from the Earth's upper atmosphere are sometimes highly variable, which can result in incomplete background removal when using simple pair subtraction. To remove this background residual, a polynomial was fitted to the sky windows above and below the object spectrum and removed from the object frames. The one-dimensional spectra of Trojans and standard stars were finally extracted from the two-dimensional images by summing up the pixel values across an aperture. The widths of the apertures were defined based on the size of the seeing disk. Usually, ground-based near-infrared spectroscopy is greatly contaminated by the strong and variable telluric absorptions. To remove these strong absorption features from atmospheric oxygen and water vapor, a spectrum of a "telluric standard star" taken close in time and air mass to the scientific target was observed and divided out from each object spectrum. We chose G-type stars, which have similar spectral slopes to the G2 V Sun, as the standard stars. These stars were selected from the UKIRT bright G star list[1] for UKIRT observations. A standard star locator (Vacca et al. 2003) was used to select nearby G stars for IRTF observations. Therefore, the telluric correction and the calibration of the asteroids' relative reflectance to the Sun could be achieved with the same division. The difference between the air mass of the target asteroid and the air mass of the standard star was selected to be as small as practical, typically less than 0.1 air mass.

[1] See http://www.jach.hawaii.edu/UKIRT/astronomy/calib/spec_cal/dwarf.html#gdwarf.

3. ANALYSIS

3.1. (*4709*) *Ennomos*

As shown in Figure 1, despite its atypical albedo, the spectrum of Ennomos appears to be featureless, with a moderately red spectral slope and no evidence for absorption bands near 1.5 or 2.0 μm that could be attributed to water ice.

We estimated the maximum allowable quantity of water ice on Ennomos in three ways. In the first method, we assume that the surface is composed of two materials and use only the albedo as the observational constraint. A fraction of the surface, f_i, is supposed to be occupied by pure water ice of albedo $p_i = 0.8$. The remainder is occupied by a dark surface of albedo $p_d = 0.04$, the average albedo of all the Trojans. Then the average albedo is

$$p_i f_i + p_d(1 - f_i) = \bar{p}.$$

With $\bar{p} = 0.13 \pm 0.02$, we solve to find $f_i = 0.12$. This simple two-component model shows that the areal fraction of clean surface water ice on Ennomos is at the level of ~10%. Of course, the model is simplistic, and a much larger fraction of *dirty* water ice could exist, while still satisfying the measured albedo.

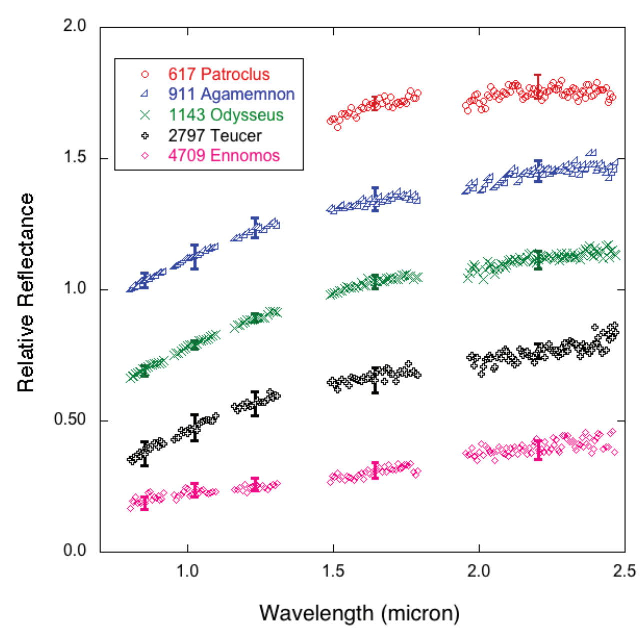

Fig. 1.—Average spectra of (4709) Ennomos, (617) Patroclus, (911) Agamemnon, (1143) Odysseus, and (2797) Teucer. All spectra are normalized at 2.2 μm and vertically offset for clarity.

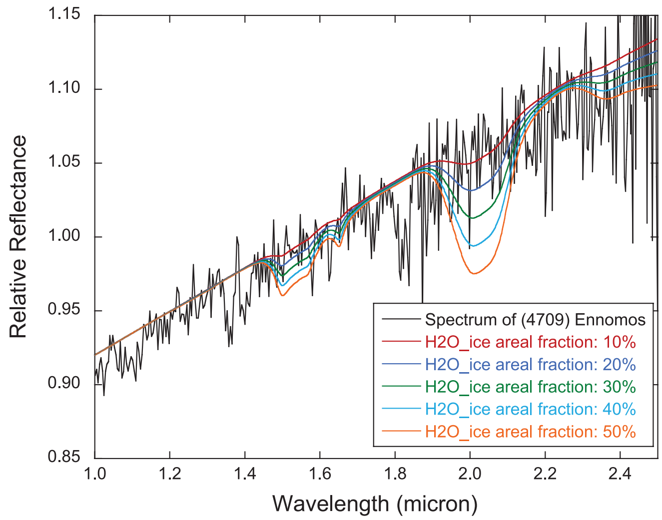

Fig. 2.—Simulated spectra with different ice fractions (*colored lines*) compared to an observed spectrum of (4709) Ennomos. The simulated spectra were computed by mixing pure water ice with reddened but spectrally featureless materials.

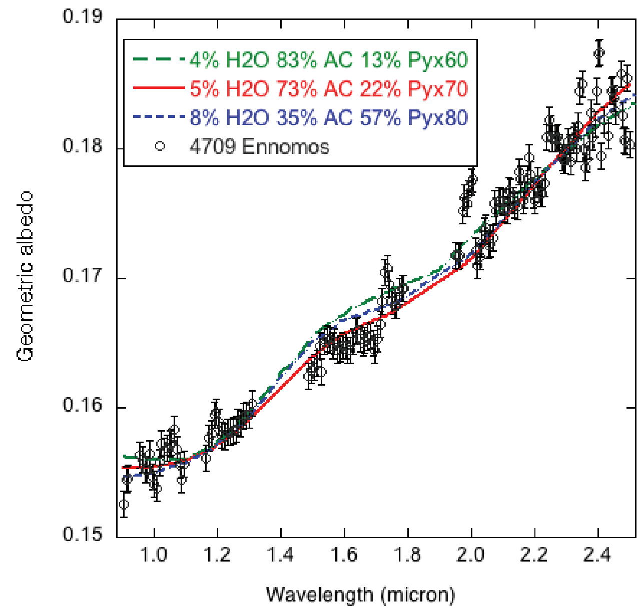

Fig. 3.—Composite spectrum of Ennomos (*circles*) extrapolated to an albedo of 0.13 in the *V* band (Fernández et al. 2003). The synthetic spectra (*colored lines*) are intimate mixtures of water ice (H_2O), amorphous carbon (AC), and pyroxene (Pyx) particles with varying weight fractions of each component, as described in the text. Pyroxenes with different Mg content (from 60% to 80%) were used, which are shown as Pyx60, Pyx70, and Pyx80.

In the second method, a similar area-mixing calculation was applied to the depth of the water ice bands at 1.5 and 2.0 μm. We reason that these absorptions, if present, must be diluted by contamination with a spectrally bland (i.e., reddened but otherwise featureless) material. We calculated the reflectance spectrum of water ice from the laboratory optical constants (Grundy & Schmitt 1998). The absorption-band shapes, depths, and centers are dependent on the assumed ice temperature (Grundy & Schmitt 1998). We used a temperature of 120 K, roughly the blackbody equilibrium temperature of objects at 5 AU. Simulated area-mixed spectra show that water ice occupying 10% or less of the surface area would be undetectable in our current observations (see Fig. 2). Therefore, although the characteristic absorption bands are absent in our data, the possible existence of a surface water ice component could be up to 1/10 of the Ennomos surface. This estimate, while similar to the constraint independently obtained from the average albedo, is limited in value by the assumption that the ice and bland absorber spectra can be linearly combined, leading us to consider the third method.

In the third method, we used an intimate mixture model kindly provided to us by Ted Roush. This code calculates the wavelength-dependent geometric albedo spectrum of our model mixtures using Hapke's formalism (Hapke 1981, 1993) assuming isotropic scattering from all grains. The details of this method are described in Roush et al. (1990) and Roush (1994). The advantage of the model is that it more accurately treats the combined effects of scattering from the high-albedo ice component with the absorption due to nonice. We adopted three compositionally distinct components to fit the spectra of Ennomos, namely, water ice, amorphous carbon, and Mg-Fe pyroxene. The optical constants of water ice are from Grundy & Schmitt (1998), the optical constants of pyroxene ($Mg_{(x)}Fe_{(1-x)}SiO_3$, $x = 0.4$–1.0) are from Dorschner et al. (1995), while those for amorphous carbon are from Rouleau & Martin (1991). We choose pyroxene rather than widely used organic materials as the reddening agent in our model for two reasons. First, the thermal emission spectra of (624) Hektor, (911) Agamemnon, and (1172) Aneas show features near 10, 18, and 28 μm that indicate fine-grained silicates on the surfaces of these bodies (Emery et al. 2006). Second, and more importantly, both Emery & Brown (2004) and Cruikshank et al. (2001) demonstrated that Mg-rich pyroxene provides a satisfactory spectral modeling component for the near-IR reflectance spectra of Trojans. Emery & Brown (2004) found that low-Fe pyroxenes tend to have high albedos. Therefore, we used Mg-rich (or Fe-poor) pyroxenes with 60%, 70%, and 80% Mg, as shown in Figure 3. Our model succeeded in simulating reflection spectra of Ennomos when the pyroxene consists of 70% Mg and 30% Fe. However, the use of these particular materials in our model is arbitrary to some extent. Any slightly red but spectrally featureless components that are mixed with an absorber and a small amount of water ice could produce similarly acceptable fits.

Our intimate mixing calculations again show that the water component can be no more than $\sim$10% by mass (Fig. 3). A smaller ice fraction could be present and contribute to the higher than average albedo of Ennomos, while eluding spectroscopic detection. Alternatively, the surface of Ennomos could be completely ice-free.

3.2. (*617*) *Patroclus*

Emery & Brown (2003) reported an absorption band in (617) Patroclus at 2.3 μm. We observed Patroclus using the UKIRT telescope on UT 2006 April 7 and 8. A total of 32 spectra, with 240 s exposure each, were obtained. However, spectra obtained on April 8 suffered from variable sky conditions and so were rejected from further analysis. Here we focus on the data from April 7 to search for potential features in the *K* band. As shown in Figure 4 (*left*), the band at 2.3 μm reported by Emery & Brown (2003) is not seen in our data. For comparison, the spectra are replotted in Figure 4 (*right*), along with the transmission spectrum of the Earth's atmosphere. The reported band is close in wavelength to a telluric feature at 2.3 μm. Several organic compounds and hydrocarbon ices, such as CH_4, C_2H_2, and $C_2H_4C_2H_6$, can produce diagnostic signatures around 2.2–2.3 μm due to the combinations of fundamental stretching modes of the C-H bond (Dotto et al. 2003). However, the surface temperature of Patroclus is probably too high for the more volatile of these materials to

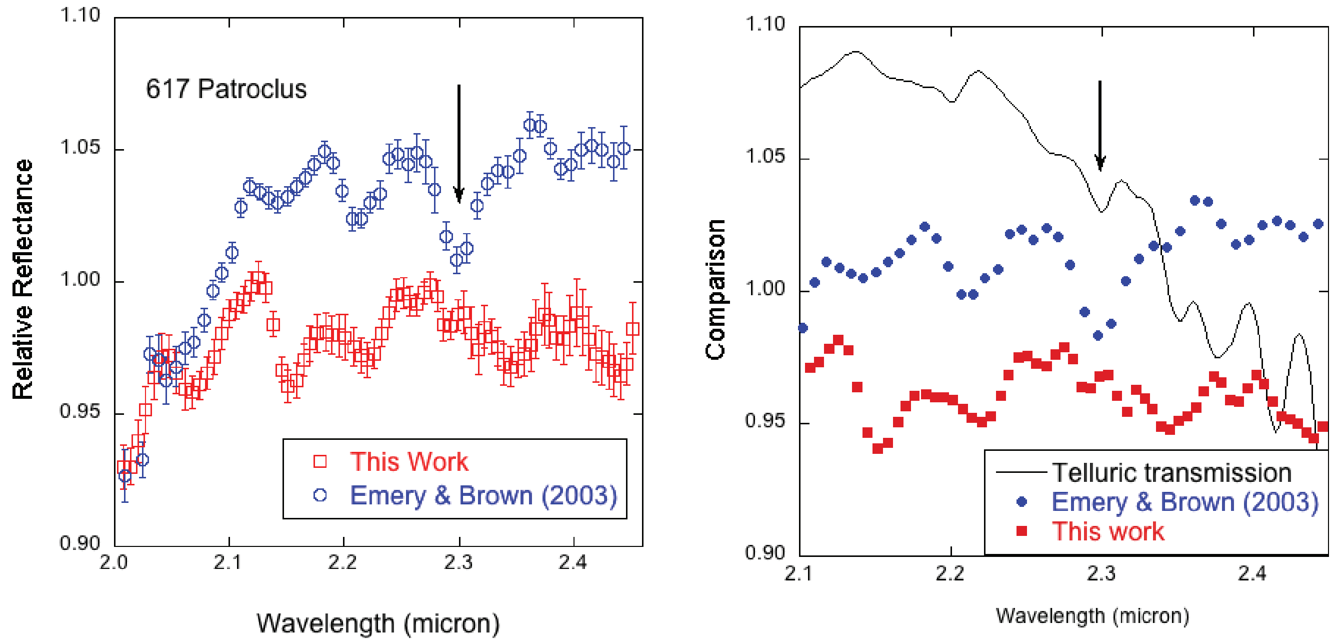

Fig. 4.—*Left*: Comparison between our observations (*red squares*) and the data from Emery & Brown (2003; *blue circles*). The arrow points out the reported absorption feature near 2.3 μm. *Right*: The transparency spectrum of the atmosphere above Mauna Kea, generated using the ATRAN modeling software (Lord 1992) and shifted for clarity. The data for the atmosphere are adopted from Gemini Observatory.

survive. Also, the first overtone of methane and acetylene should produce an absorption feature around 1.7 μm (Moroz et al. 1998), which was not reported by Emery & Brown (2003). Therefore, we suspect the weak absorption at 2.3 μm is probably a residual from incomplete telluric calibration.

Nevertheless, both our spectrum and Emery's spectrum contain several structures between 2.0 and 2.5 μm. Few of the features are reproducible, and we presume that they are due to poor telluric calibration or perhaps to an instrumental cause. The sharp absorption at 2.01 μm in Figure 4 (*left*) appears in both our spectrum and that of Emery & Brown. However, it coincides with the telluric CO_2 band, and the spectrum of the standard star also shows this strong absorption. Therefore, the 2.01 μm feature is unlikely to be intrinsic. Other features near 2.21 and 2.35 μm could also be manifestations of atmospheric absorption.

3.3. (*1143*) *Odysseus*

Trojan (1143) Odysseus was observed twice in 2006 June and August using Spex and UIST, respectively. The two data sets on this object match well with a spectral slope similar to that shown in Figure 5. However, the reported 1.7 μm feature (Emery 2002) is not present in either IRTF or UKIRT spectra. This object appears to be spectrally red and featureless in the 0.8–2.5 μm range (see Fig. 1).

3.4. (*911*) *Agamemnon*

According to Emery (2002) there is a hint of a weak feature near 1.7 μm in this object. As discussed in § 3.2, the 1.7 μm absorption could be due to the C-H bond in hydrocarbons. These hydrocarbon molecules would also absorb radiation at $\sim$2.3 μm and produce stronger features in the *K* band (Emery 2002). However, our observations show neither 1.7 nor 2.3 μm absorptions (see Fig. 6). Agamemnon is suggested to contain a sharp absorption at 3.21 μm (Emery 2002), which, however, is beyond the wavelength coverage of our data. Thus, further observations are needed to confirm the 3 μm feature.

3.5. (*2797*) *Teucer*

Trojan (2797) Teucer is reported to exhibit two features in the *H* and *K* bands (Emery 2002); a hint of 1.7 μm absorption and a broad double-lobed feature in the 2.28–2.40 μm region, respectively. Our observations (Fig. 7) of Teucer show a flat and featureless spectrum in the region of 1.5–1.8 μm with no sign of possible absorption. For the *K* band, both our spectra and Emery's spectra contain several structures that are likely to be

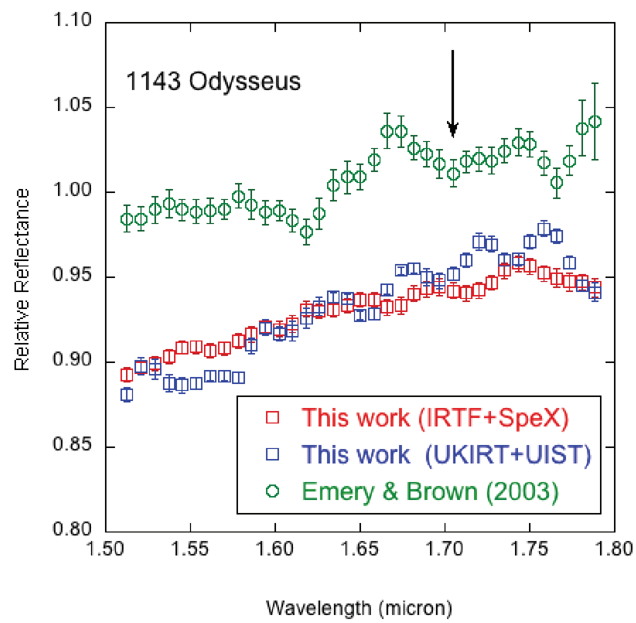

Fig. 5.—Comparison between our data (*squares*) and data from Emery & Brown (2003; *green circles*). The red squares represent data taken with UIST, while blue squares are the data taken with Spex. The arrow points out the reported absorption feature near 1.7 μm. There is a strong absorption present near 1.62 μm in the green spectrum, which is not intrinsic but a contamination from telluric absorption.

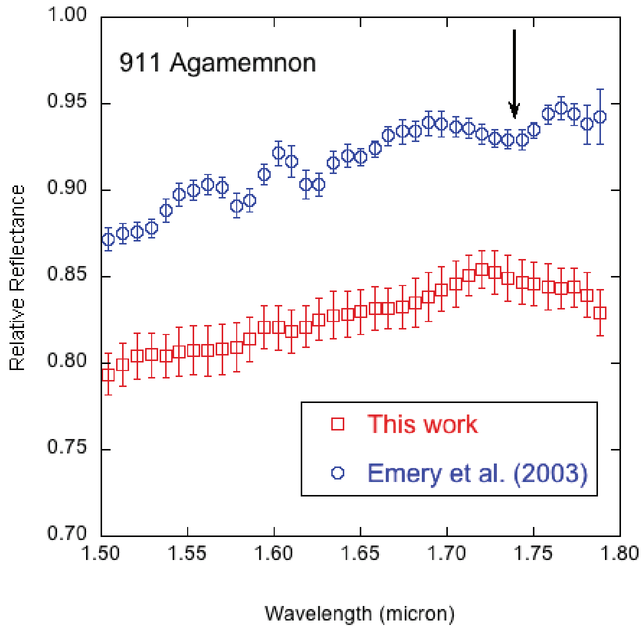

FIG. 6.—Comparison between the data described in the text (*red square*) and the data from Emery & Brown (2003; *blue circle*). The arrow points out the reported absorption feature near 1.73 μm.

manifestations of the increased noise level. Near 2.35 μm (see Fig. 7) there is a broad absorption; however, it is a single-peak feature and does not align well with the claimed 2.3 μm feature.

4. DISCUSSION

Our observations show no sign of water ice in the spectra of the bright Trojan (4709) Ennomos. Moreover, we do not confirm the intriguing 1.7 and 2.3 μm absorption features noted by Emery & Brown (2003). As shown in Figure 1, all five Trojans exhibit featureless spectra with typical neutral to red spectral slopes. We noted that the spectrum of Ennomos is distinctively flatter than others, which could be due to recent collisions that liberated materials from subsurface layers (Luu & Jewitt 1996) or recondensation of gas and dust after temporary cometary activity (Luu et al. 2000). The high albedo and an almost neutral spectral slope both hint at a possible resurfacing process that recently modified the surface of Ennomos. Therefore, further observations of Ennomos are needed not only to investigate its surface properties but also to search for unusual materials possibly from its interior.

Although we find no evidence of water ice in the spectrum of Ennomos, this object could still be icy provided the band depths are reduced considerably by absorbing matter (e.g., organics). Early work (Clark & Lucey 1984) showed that a few percent (by weight) of absorbing materials mixed with pure water ice can weaken the 1.5 and 2.0 μm features, making them undetectable. However, water ice has a much stronger absorption band near 3.1 μm, and a pioneering study by Jones (1988) showed that even a large fraction of opaque materials could not mask this stronger band. Furthermore, common molecular bonds (i.e., O-H, C-N, and N-H) produce diagnostic absorption features in this region. Observations at 3 μm could probe (4709) Ennomos for water and many other interesting materials. Unfortunately, 3 μm observations are among the most challenging of any possible from the ground, while no space-based telescopes currently offer sensitivity at this wavelength.

In order to determine surface composition and constrain possible surface components for spectral models, diagnostic detections are crucial. However, atmospheric contamination from incomplete telluric calibration could easily produce features at these diagnostic wavelengths. To distinguish an intrinsic feature from an atmospheric artifact, multiple observations of the target using different telluric standard stars are necessary. Furthermore, overtone and combination bands of water molecule/organic molecules would produce multiple diagnostic absorptions in the near-infrared. Thus, the presence of multiple diagnostic features of a component material at the correct wavelengths could be taken as conclusive evidence of its existence.

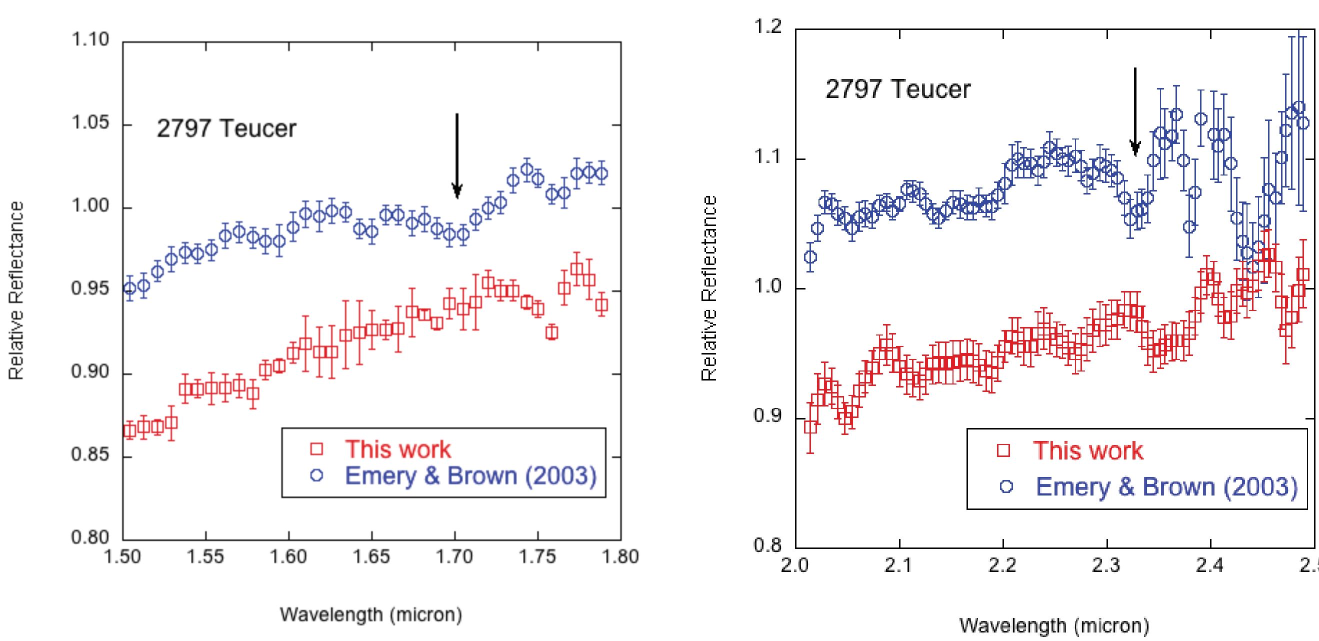

FIG. 7.—Comparison between the data described in the text (*red squares*) and the data from Emery & Brown (2003; *blue circles*). The arrow points out the absorption features reported near 1.73 (*left*) and 2.3 μm (*right*).

5. SUMMARY

1. The near-infrared reflection spectrum of the high-albedo Trojan (4709) Ennomos is slightly red but otherwise spectrally featureless.

2. Three models applied to the Ennomos spectrum indicate that water ice occupies no more than 10% of the surface area.

3. Spectral features reported earlier on Trojans (617) Patroclus, (911) Agamemnon, (1143) Odysseus, and (2797) Teucer are not confirmed in our data.

We would like to thank Joshua Emery for generously providing original data from the paper by Emery & Brown (2003), and we thank Ted Roush for kindly providing the intimate mixture model. We thank Scott Sheppard for providing the IRTF spectra of (4709) Ennomos. We acknowledge James Bauer for fruitful suggestions and discussions about spectral modeling and Rachel Stevenson and Pedro Lacerda for kindly reading the manuscript. We thank the anonymous referee for valuable comments to improve the manuscript. This work is supported by grant NNG 06GG08G to David Jewitt from the NASA Planetary Origins program.

REFERENCES

Brown, R. H., Cruikshank, D. P., Pendleton, Y. J., & Veeder, G. J. 1997, Science, 276, 937
Ciesla, F. J., & Cuzzi, J. N. 2006, Icarus, 181, 178
Clark, R. N., & Lucey, P. G. 1984, J. Geophys. Res., 89, 6341
Cruikshank, D. P., Dalle Ore, C. M., Roush, T. L., Geballe, T. R., Owen, T. C., de Bergh, C., Cash, M. D., & Hartmann, W. K. 2001, Icarus, 153, 348
Cruikshank, D. P., et al. 1998, Icarus, 135, 389
Davies, J. K., Roush, T. L., Cruikshank, D. P., Bartholomew, M. J., Geballe, T. R., Owen, T., & de Bergh, C. 1997, Icarus, 127, 238
Doressoundiram, A., Barucci, M. A., Tozzi, G. P., Poulet, F., Boehnhardt, H., de Bergh, C., & Peixinho, N. 2005, Planet. Space Sci., 53, 1501
Dorschner, J., Begemann, B., Henning, T., Jaeger, C., & Mutschke, H. 1995, A&A, 300, 503
Dotto, E., Barucci, M. A., & de Bergh, C. 2003, Earth Moon Planets, 92, 157
Dumas, C., Owen, T., & Barucci, M. A. 1998, Icarus, 133, 221
Emery, J. P. 2002, Ph.D. thesis, Univ. Arizona
Emery, J. P., & Brown, R. H. 2003, Icarus, 164, 104
———. 2004, Icarus, 170, 131
Emery, J. P., Cruikshank, D. P., & van Cleve, J. 2006, Icarus, 182, 496
Fernández, Y. R., Sheppard, S. S., & Jewitt, D. C. 2003, AJ, 126, 1563
Fleming, H. J., & Hamilton, D. P. 2000, Icarus, 148, 479
Fornasier, S., Dotto, E., Marzari, F., Barucci, M. A., Boehnhardt, H., Hainaut, O., & de Bergh, C. 2004, Icarus, 172, 221
Grundy, W. M., & Schmitt, B. 1998, J. Geophys. Res., 103, 25809
Hapke, B. 1993, Theory of Reflectance and Emittance Spectroscopy (Cambridge: Cambridge Univ. Press)
———. 1981, J. Geophys. Res., 86, 3039
Jewitt, D. C., & Luu, J. 2004, Nature, 432, 731
———. 1990, AJ, 100, 933
Jones, T. D. 1988, Ph.D. thesis, Univ. Arizona
Jones, T. D., Lebofsky, L. A., Lewis, J. S., & Marley, M. S. 1990, Icarus, 88, 172
Kawakita, H., Watanabe, J.-I., Ootsubo, T., Nakamura, R., Fuse, T., Takato, N., Sasaki, S., & Sasaki, T. 2004, ApJ, 601, L191
Lebofsky, L. A., Jones, T. D., Owensby, P. D., Feierberg, M. A., & Consolmagno, G. J. 1990, Icarus, 83, 16
Lebofsky, L. A., & Spencer, J. R. 1989, in Asteroids II, ed. R. P. Binzel, T. Gehrels, & M. S. Matthews (Tucson: Univ. Arizona Press), 128
Lord, S. D. 1992, NASA Tech. Rep. 103957 (Moffett Field: NASA Ames Research Center)
Luu, J., & Jewitt, D. 1996, AJ, 112, 2310
Luu, J., Jewitt, D., & Cloutis, E. 1994, Icarus, 109, 133
Luu, J., Jewitt, D., & Trujillo, C. 2000, ApJ, 531, L151
Morbidelli, A., Levison, H. F., Tsiganis, K., & Gomes, R. 2005, Nature, 435, 462
Moroz, L. V., Arnold, G., Korochantsev, A. V., & Wasch, R. 1998, Icarus, 134, 253
Moroz, L., Baratta, G., Strazzulla, G., Starukhina, L., Dotto, E., Barucci, M. A., Arnold, G., & Distefano, E. 2004, Icarus, 170, 214
Pollack, J. B., Hubickyj, O., Bodenheimer, P., Lissauer, J. J., Podolak, M., & Greenzweig, Y. 1996, Icarus, 124, 62
Ramsay Howat, S. K., et al. 2004, Proc. SPIE, 5492, 1160
Rayner, J. T., Toomey, D. W., Onaka, P. M., Denault, A. J., Stahlberger, W. E., Vacca, W. D., Cushing, M. C., & Wang, S. 2003, PASP, 115, 362
Rouleau, F., & Martin, P. G. 1991, ApJ, 377, 526
Roush, T. L. 1994, Icarus, 108, 243
Roush, T. L., Pollack, J. B., Witteborn, F. C., Bregman, J. D., & Simpson, J. P. 1990, Icarus, 86, 355
Stevenson, D. J., & Lunine, J. I. 1988, Icarus, 75, 146
Vacca, W. D., Cushing, M. C., & Rayner, J. T. 2003, PASP, 115, 389